THE TOP-DOWN MECHANISM FOR BODY-MASS–ABUNDANCE SCALING

A. G. Rossberg,[1,2,4] R. Ishii,[3] T. Amemiya,[1] and K. Itoh[1]

[1]*Yokohama National University, Graduate School of Environment and Information Sciences, Yokohama 240-8501 Japan*
[2]*International Institute for Applied Systems Analysis, 2361 Laxenburg, Austria*
[3]*Frontier Research Center for Global Change, JAMSTEC, Yokohama 236-0001 Japan*

Abstract. Scaling relationships between mean body masses and abundances of species in multitrophic communities continue to be a subject of intense research and debate. The top-down mechanism explored in this paper explains the frequently observed inverse linear relationship between body mass and abundance (i.e., constant biomass) in terms of a balancing of resource biomasses by behaviorally and evolutionarily adapting foragers, and the evolutionary response of resources to this foraging pressure.

The mechanism is tested using an allometric, multitrophic community model with a complex food web structure. It is a statistical model describing the evolutionary and population dynamics of tens to hundreds of species in a uniform way. Particularities of the model are the detailed representation of the evolution and interaction of trophic traits to reproduce topological food web patterns, prey switching behavior modeled after experimental observations, and the evolutionary adaptation of attack rates. Model structure and design are discussed.

For model states comparable to natural communities, we find that (1) the body-mass–abundance scaling does not depend on the allometric scaling exponent of physiological rates in the form expected from the energetic equivalence rule or other bottom-up theories; (2) the scaling exponent of abundance as a function of body mass is approximately −1, independent of the allometric exponent for physiological rates assumed; (3) removal of top-down control destroys this pattern, and energetic equivalence is recovered. We conclude that the top-down mechanism is active in the model, and that it is a viable alternative to bottom-up mechanisms for controlling body-mass–abundance relations in natural communities.

Key words: abundance; allometric scaling; body mass; community models; food webs.

INTRODUCTION

Empirical data show the abundances, N, and the mean body masses, M, of species related by power laws of the form $N \approx N_0(M/M_0)^{-1+\lambda}$, where one can set $M_0 = 1$ kg by convention and $|\lambda|$ is usually small compared to one (e.g., Sheldon et al. 1972, Damuth 1981, Rodriguez and Mullin 1986, Nee et al. 1991, Carbone and Gittleman 2002, Marquet 2002, Cohen et al. 2003, Quiñones et al. 2003, Marquet et al. 2005, Mulder et al. 2005). The precise value of λ varies and depends on the precise question asked (Sprules and Munawar 1986, Brown et al. 2004, Li et al. 2004, Marquet et al. 2005). For stable pelagic ecosystems across trophic levels (e.g., Sheldon et al. 1972, Rodriguez and Mullin 1986, Sprules and Munawar 1986, Gaedke 1992, Cohen et al. 2003, Quiñones et al. 2003), and to some degree also for soil food webs (Mulder et al. 2005), the pattern is particularly clear, with $\lambda \approx 0$. These observations suggest four questions: (1) What are the mechanisms that lead to the power laws? (2) What are the values of λ implied by these mechanisms? (3) What determines the

value of N_0? (4) And what determines the observed scatter by a factor 10–100 up and down around the power laws (Cyr 2000)? The last question seems to be at the core of the problem of understanding species abundance distributions (Whittaker 1965, Cyr 2000) and shall here be set aside, leaving questions 1–3.

Many theories for the origin of the power laws build on the "energetic equivalence" (Nee et al. 1991) between species of different size, first observed by Damuth (1981) for herbivorous mammals. The conceived mechanism is fundamentally bottom-up: for physiological reasons, mass-specific metabolic rates scale as M^{ζ_r}, and rates per individual as $M \times M^{\zeta_r} = M^{1+\zeta_r}$ with $\zeta = -1/4$. Thus, an assumed fixed rate R of energy supply can support at most $N \sim R/M^{1+\zeta_r}$ individuals, yielding $-1 + \lambda = -1 - \zeta_r$ and $\lambda = -\zeta_r \approx 1/4$. Advanced bottom-up theories (e.g., Platt and Denman 1977, 1978, Cyr 2000, Brown et al. 2004, Meehan 2006) take losses by the transfer of energy from one trophic level to the next into account and arrive, by a combination of quantities such as trophic and metabolic efficiencies and predator–prey mass ratios at $\lambda \approx 0$ or other values. Characteristic the whole class of bottom-up theories is that they predict λ to be of the form $\lambda = \lambda_0 - \zeta_r$, with λ_0 independent of ζ_r. That is, a change in the allometric exponent for the metabolic rate

would lead to a change of equal size for λ, but with the opposite sign.

Criticism of bottom-up theories of this form (Griffiths 1992, Currie 1993, Marquet et al. 1995, Blackburn and Gaston 1999) has pointed out that the nature of the uniform source of energy is left unclear, and that the theories do not explained why this source would provide the same amount of energy to each species at a given trophic level. Leaving this point open, it has been argued (e.g., Blackburn and Gaston 1999), renders the theories somewhat vacuous.

The review by Blackburn and Gaston (1999) discusses five more mechanisms that have been proposed for body-mass–abundance scaling. Three of them relate to observational effects, two to ecological mechanisms. But none of these seems to be strong enough to explain the observed scaling over 10 or more orders of magnitude and a large range of taxa. Duarte et al. (1987) considered limitations of space as the mechanism underlying body-mass–abundance scaling. However, the space left between individuals, e.g., in the pelagic communities of the open oligotrophic waters of the ocean (Rodriguez and Mullin 1986, Quiñones et al. 2003), often seems to be too large for this mechanism to become effective.

Yet another conceivable mechanism had been shortly mentioned by Peters (1983), but seems to have received only little attention since: the biomasses of species might be balanced by consumers to be all of similar size. Thus $B = M \times N \approx$ constant and $\lambda = 0$. This explanation is fundamentally top down. Intuitively the idea is clear: if there was a species with an outstanding large (eatable) biomass, many consumers would adapt their behavior or evolve to feast on it, thus bringing this species back to the normal biomass level or driving it into extinction.

Some indications for this mechanism to be feasible can be found from the model of Benoît and Rochet (2004), which describes size-dependent trophic interactions within a community modeled by a continuous size spectrum. Benoît and Rochet find $\lambda \approx 0$ nearly constant while varying parameters, including ζ_r. However, in a model by Loeuille and Loreau (2006), which differs from that of Benoît and Rochet among others by resolving individual species and allowing body masses to evolve, λ depends strongly on model parameters. Also, Damuth (2007) recently interpreted simulations using a simple model of competition for energy on evolutionary time scales as supportive for the bottom-up mechanism. The question is therefore not so much if the top-down mechanism works in principle, but if it will be active under realistic conditions.

In the following section, we will first introduce a general model of multitrophic community structure appropriate for studying this question. In order to reduce the dependence of model results on questions whether particular model elements affect the relevant mechanism for body-mass abundance scaling, which is a priori difficult to answer, and to make the model more realistic while maintaining generality, construction of

the model was lead by the principle to include ideally all those elements that are common across a broad range of ecosystems, preferentially those that are empirically well studied. In particular, all elements contained in the three models discussed above by Benoît and Rochet, Loeuille and Loreau, and Damuth are taken into account, except for ontogenetic growth (Benoît and Rochet). Since the model is rather complex, a detailed description of the model and discussions of parameterization and model design have been referred to the Appendix.

After discussing and comparing several aspects of model community structure with empirical data (*General properties of model communities and their dynamics*), we demonstrate in *Numerical experiments and results* that, in the model, the prediction $\lambda = \lambda_0 - \zeta_r$ of bottom-up theories does not hold. Rather, we find $\lambda \approx 0$ independent of ζ_r. Next, we confirm the presence of the top-down mechanism by comparing the model with variants where top-down effects have been artificially removed. We then present a detailed discussion of how the top-down mechanism works. Based on these results, a simple formula can be set up that, up to a factor ≈ 100, predicts the abundance of arbitrary consumer species in a community in terms of physiological properties of individual species.

THE POPULATION-DYNAMICAL MATCHING MODEL

Overall model structure

A list of elements included in the model and references motivating their implementation are given in Table 1. The main problem targeted by the model is to describe the structure and population dynamics of a multitrophic community at a single location. However, it turns out that, in order to obtain more realistic community structures, it is useful to model, in a simplified form, the evolutionary history of this community and the structure of other communities from which species may invade.

Hence, our model describes the population dynamics and evolution of four communities, which are weakly coupled by the occasional exchange of species, but population-dynamically uncoupled. It is a statistical model describing tens to hundreds of species in a uniform way. Only "producers" (e.g., algae or plants) and "consumers" (all higher trophic levels) are explicitly distinguished. Since, for reducers in the soil, energy (detritus) is provided largely independent of consumption, just as light for primary producers, reducers in soil ecosystems can take the role of "producers" in the model as well. Each community is characterized by the biomasses B_i and the mean body masses M_i of its member species i, implying population numbers $N_i = B_i/M_i$, and by the trophic interaction structure.

Evolution

On time scales larger than typical population-dynamical times, the species pool of each community evolves—technically by "speciations," local extinctions, and

TABLE 1. Elements contained in the population-dynamical matching model.

Model element	Based on
Energy conservation and dissipation	McNiel and Lawton (1970), Peters (1983)
Allometric scaling of physiological rates	McNiel and Lawton (1970), Peters (1983), Savage et al. (2004)
Type II functional responses	Jeschke et al. (2004)
Prey switching	Greenwood and Elton (1979)
Size ratios determining trophic links	Claessen et al. (2002), Brose et al. (2006)
Abstract traits determining trophic links	Yoshida (2003), Rossberg et al. (2006a)
Evolution of body masses	Loeuille and Loreau (2005)
Evolution of abstract traits	Yoshida (2003), Rossberg et al. (2006a)
Differentiation of evolution rates by traits	Rossberg et al. (2006a), Bersier and Kehrli (2008)
Community evolution through simplified speciations	see *The population-dynamical matching model: Evolution* and Caldarelli et al. (1998)
Population-dynamically isolated, evolutionary coupled patches	arguments discussed in *The population-dynamical matching model: Evolution*
Free evolution of attack rates	arguments discussed in *The population-dynamical matching model: Attack rates*

"invasions" from the three other communities. However, the picture behind these processes, sketched in Fig. 1, is more complex: each of the four explicitly modeled communities (black "lakes" in Fig. 1) has a number of similar communities in its vicinity that are not explicitly modeled (gray "lakes"). Most speciations are allopatric and occur within these surrounding communities, at times and for reasons unrelated to the explicitly modeled communities. But species invading a modeled community from its surroundings will often have some similarity with species already present due to common evolutionary ancestors. Thus, from the perspective of the local community, such invasions will appear as if they were spontaneous "speciations" of existing species by large mutations. Furthermore, "invasions" from the other three modeled communities (arrows in Fig. 1) proceed in steps through other systems, thus giving rise to some evolutionary variation and some delay, and decoupling the population dynamics of the four modeled

communities. Thus, "speciations" and "invasions" in the model are extremely coarse-grained descriptions of the actual evolutionary processes. It can be shown that this coarse graining of phylogeny in models of local communities affects food web topology only weakly (Rossberg 2008). Except for some sympatric speciations, both local "speciations" and "invasions" correspond, in reality, to invasions of the community by species more or less related to existing ones. We shall denote these processes below collectively as additions to a community, and use the number of species added (abbreviated as "sa") as a measure of evolutionary time.

Attack rates

Traits mutating in speciations include not only body masses and abstract foraging and vulnerability traits, which together determine feeding relationships, but also the attack rates of consumers. Attack rates can evolve freely in the model without an explicit physiological
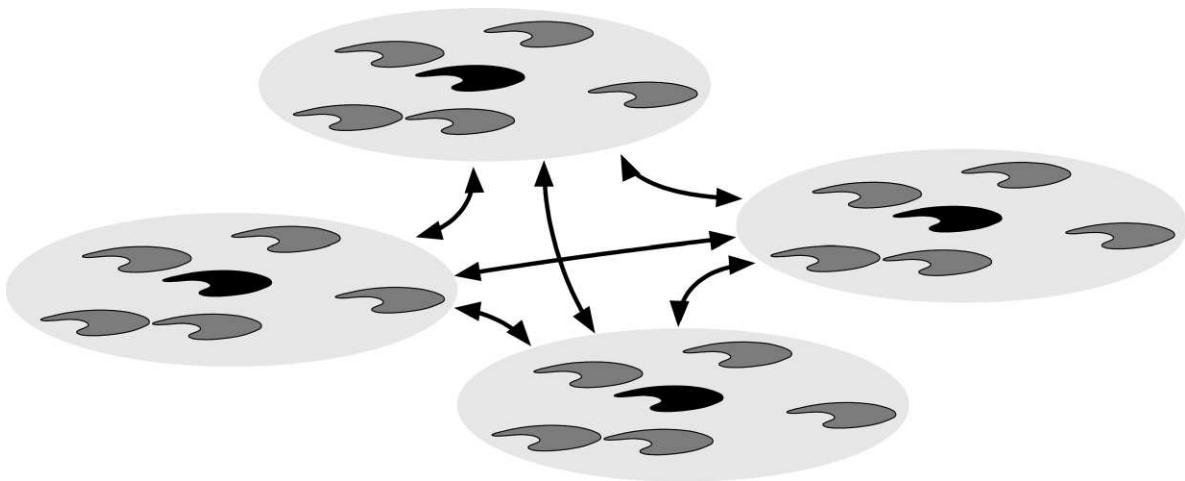

FIG. 1. The hierarchical spatial structure assumed in the evolutionary submodel. Black "lakes" represent the four explicitly modeled communities; gray "lakes" represent similar communities in the vicinity that are not explicitly modeled. Arrows represent "invasions" from the other three modeled communities. See *The population-dynamical matching model: Evolution* for more detailed discussion.
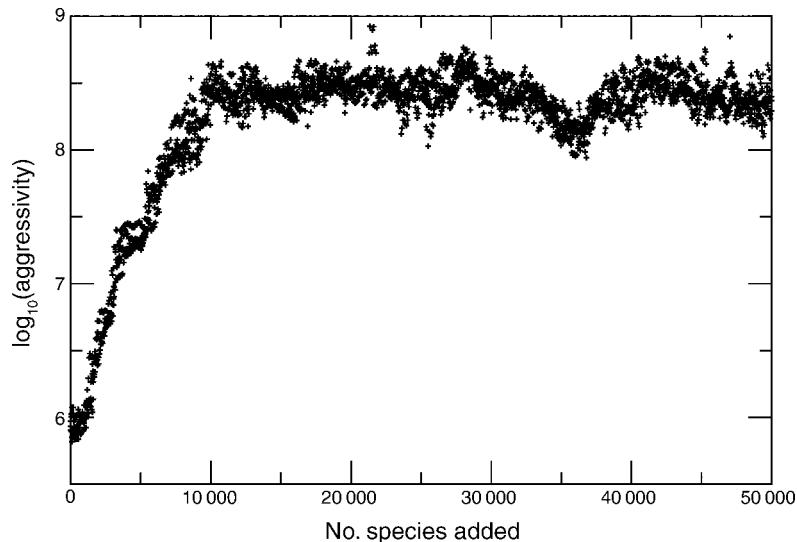
FIG. 2. Time series of the mean consumer aggressivity, g, the attack rate normalized to consumer respiration rate and system area (g has units of m^2/kg). Samples (plus signs) are taken in each community after every 60 sa (species added).

trade-off. As is shown below, mean attack rates of communities will nevertheless evolve to some stable value, well below the point of total eradication of all producers, but sufficiently large to control resource populations. This is not to imply that attack rates in nature cannot also be determined by physiological and physical constraints, but this mechanism is here excluded for simplicity.

Parameterization

Empirical estimates for model parameters were used whenever possible, and model variables are expressed in physical units. This allows a quantitative comparison of macroecological model properties (e.g., biomass densities) with empirical data. If there was a choice, we preferred parameter values applicable to pelagic communities, because (1) for pelagic communities the empirical pattern of body-mass–abundance scaling is particularly clear; (2) due to their relatively high spatial homogeneity, they might be comparatively easy to model; and (3) in the present form the model favors primary producers of small body mass resembling phytoplankton (see, however, *Numerical experiments and results: Testing the top-down theory for body-mass–abundance scaling: Communities without consumers*). Interpretations of model states in terms of pelagic communities therefore come easily to mind, and we shall sometimes invoke them below. Yet, in order to maintain generality, the model was intentionally constructed such as not to include elements specific to and should not be misunderstood as an attempt to quantitatively reproduce the properties of particular community types.

Masses are expressed in the currency of wet biomass, and biologically available energy is assumed proportional to mass, since this is the traditional choice of allometric theory (Peters 1983). This choice obviously

raises some conceptual and quantitative issues, but at the degree of accuracy targeted here, these are not relevant, yet.

The Appendix first gives a complete definition of the model. It then provides a detailed discussion of specific model design decisions, the rational behind choices of parameter values, and a full list of model parameters and variables.

GENERAL PROPERTIES OF MODEL COMMUNITIES AND THEIR DYNAMICS

The purpose of the sections is twofold. It provides information on general model community structure that is referred to in the discussion of body-mass–abundance scaling further below, and, by comparison with empirical results, it offers a picture of the degree of realism that is reached by the model and points out possible artifacts.

Evolution of attack rates and steady state

Simulations of the model show that at the community level attack rates evolve to a stable evolutionary equilibrium. We define the aggressivity g_i of a species i as $g_i = a_i A / r_i$, i.e., as the attack rate a_i normalized to the system area A and the specific respiration rate r_i. The aggressivity has dimensions of an inverse biomass density. Fig. 2 shows a time series of the community means of the aggressivity g for standard parameters as listed in the Appendix. After a transient period with exponential growth, the aggressivity settles in at $3 \times 10^6 \pm 2 \times 10^6$ m^2/kg (mean $\pm$ SD).

After the aggressivity saturates, other system properties, such as the number of species, reach their steady-state values as well. Characterizations of the steady state in the next section are based on the data from 18 000 sa to 80 000 sa, where the simulations were stopped.
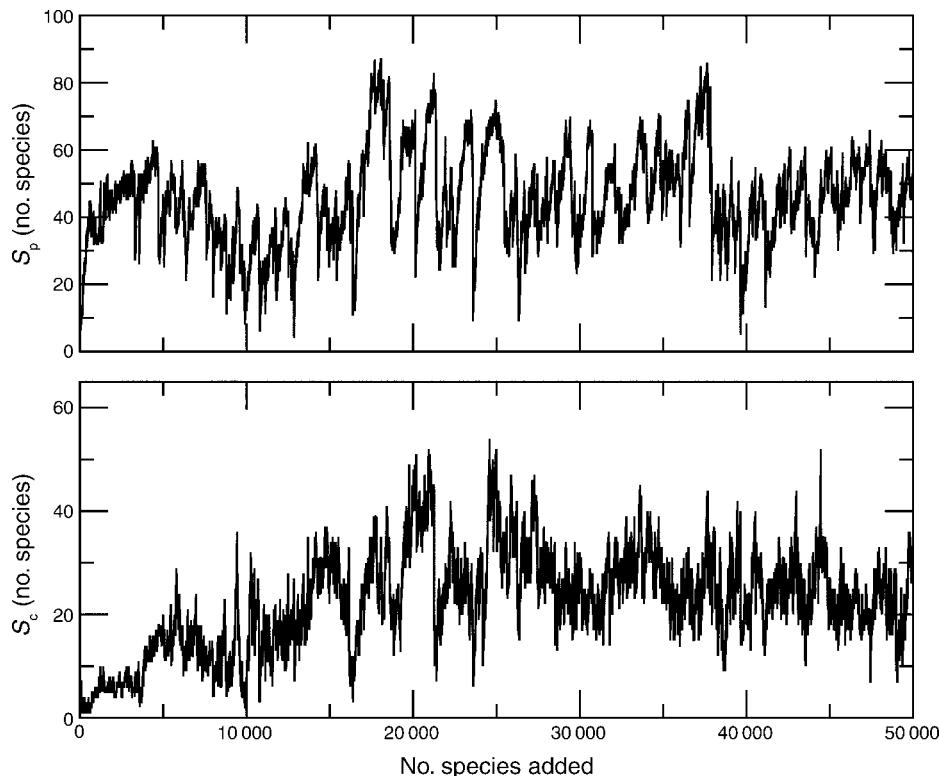
Fig. 3. Time series of the number of producer species (S_p) and the number of consumer species (S_c) in one of the four communities.

Fluctuations in the evolutionary steady state

In the steady state, each community consists of $S_p = 46 \pm 14$ producer species and $S_c = 24 \pm 8$ consumer species on the average. Fig. 3 displays the time series of S_p and S_c for one of the four communities. Immediately apparent are the strong fluctuations, which are due to intermittent extinction avalanches, not unlike those found in the paleontological record (e.g., Solé et al. 1997). Amaral and Meyer (1999) observed such extinction avalanches also in a simplified model for the evolution of food web topology. Many later models combining evolutionary and population dynamics did not produce large extinction avalanches (Drossel et al. 2001, Yoshida 2003, Loeuille and Loreau 2005, 2006). It is not clear if the avalanches found in the model correspond to those observed.

Other quantities, such as the aggressivity displayed in Fig. 2, also exhibit fluctuation over long time scales (thousands of sa). The resulting temporal correlations affect the accuracy of characterizations of the steady state, which is, e.g., reflected in the residual scatter of the simulation results for λ in Fig. 8.

Distribution of body masses

The average number of species in each logarithmic body size class is shown in Fig. 4. In the presence of herbivory, producer body masses tend to evolve toward the lowest allowed value in the model, M_{min}, of 10^{-13} kg (but see Numerical experiments and results: Testing the top-down theory for body-mass–abundance scaling: Communities without consumers for the case without herbivory). Thus, almost all producers fall into the smallest size class. The average maximum $\log_{10}$(body mass) (body mass measured kilograms) in a community is -0.5 ± 2.0. This upper limit for the body mass is partially due to the finite habitat size, and partially due to energetic or dynamic constraints along the food chain. The hard-coded upper limit of the model $M_{max} = 10^3$ kg only marginally affects this value.

In empirical data for lakes (e.g., Jonsson et al. 2005), the body masses of producer species easily span two orders of magnitude. The extremely sharp distribution found here is certainly a consequence of the sharp lower body-mass cutoff employed in the model. On the other hand, the maximum of the consumer species distribution near 10^{-9} kg has been found empirically in similar form by Jonsson et al. (2005), and the secondary peak near 10^{-2} kg, corresponding to fish species, as well, albeit sharper than here.

Typical population dynamics in the steady state

After the perturbations arising when species are added to the communities have relaxed, populations typically exhibit chaotic, and occasionally also periodic, oscillations. Due to their small body masses and the resulting
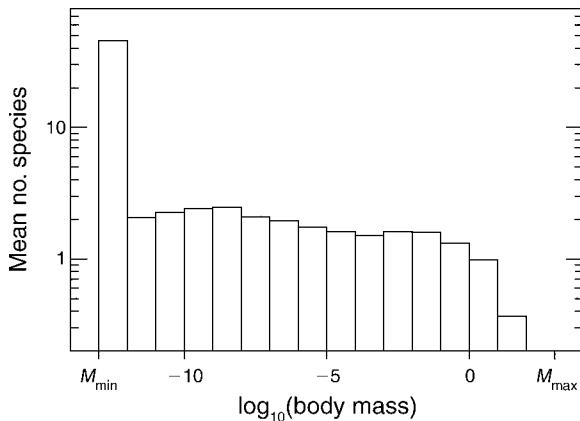
FIG. 4. Mean number of species (log scale) in each decimal size class in the model steady state, where M_{min} is the lowest value allowed in the model and M_{max} is the highest value allowed in the model. Log-transformed body mass was originally measured in kilograms.

fast population dynamics, the variability of the biomasses of producers is much larger than that for most consumers. Fig. 5 displays a typical time series for the producer biomasses in a community. Some producers appear to follow "K strategies" (small variability) others "r strategies" (algae blooms), with biomasses spanning four orders of magnitude or more (typical values of $SD(\log_{10} B_i)$ are in the range 0.5–1.5). The duration of the blooming events is on the order of weeks, compatible with observations in pelagic communities. The intensity of blooming shows no seasonal variability because seasonal effects are not modeled. Due to their larger body masses, the variability of consumer biomasses is much smaller (typically $SD(\log_{10} B_i) < 0.3$).

Results presented in the following sections always refer to time averages of biomasses B_i and trophic mass flows ($f_{ij} B_j$ in the formalism of the Appendix), obtained numerically from simulations of population dynamics.

Distribution of trophic levels

Fig. 6 shows the effective trophic level h (Levine 1980) vs. its relative rank. Specifically, the effective trophic levels of all species from all communities, sampled every 60 sa in the steady state, are ordered from large to small, and the ranks in this order are normalized by dividing by the total number of sampled species. The cumulative probability distribution can be obtained from this graph by a simple exchange of axis. This representation of the level structure was chosen for an easy comparison with the corresponding empirical result of Christian and Luczkovich (1999) for a seagrass community, who found that "The effective trophic levels of consumers tended to aggregate near integer values, but the spread from integer values increased with increasing level." The same phenomenon is found in simulations. This partially quantized structure justifies the grouping of species into trophic levels (producers, herbivores, carnivores, super-

carnivores) according to the integer value nearest to h. The average community maximum effective trophic level is $h_{max} = 3.7 \pm 0.4$ in the steady state. Effective trophic levels larger than 4.5 are rarely observed.

Topological properties of model food webs

Food web topologies were obtained by considering exactly those resources as linked to a consumer that contribute more than 1% to the consumer's diet (Drossel et al. 2004). A theoretically important property of food webs (May 1972) is the number of links per species, the link density Z. We obtained $Z = 4.1 \pm 1.3$ links per species. For a better comparison with empirical data on food web topology, Z and the topological food web properties listed in Table 2 have been computed after the following standardization of the raw topological data: first, small unconnected sub-webs are removed (Williams and Martinez 2000), then all producers are lumped into a single species, and finally species with the same sets of consumers and resources are lumped together as "trophic species" (Cohen et al. 1990) (for motivation and discussion, see Rossberg et al. 2006a).

A quantity related to Z is the average number of resources of a consumer, the consumer link density Z_c (8 $\pm$ 2 resources in the steady state). Since this quantity is directly empirically accessible without sampling a complete web (Rossberg et al. 2006b), no standardization of food web topology was done to compute it.

Large link densities, as we find them here in good accordance with empirical data (Dunne et al. 2002, Banašek-Richter et al. 2005, Rossberg et al. 2006b), are known to be difficult to reproduce in complex population-dynamical models. For example, link densities in the models investigated by Drossel et al. (2004) do not exceed 2.3. (In other work, larger values are reported, but these generally include all links regardless of their strength.) The present model would not yield large link densities either, if the known stabilizing effect of prey switching (Oaten and Murdoch 1975) had not been included. Large link densities, on the other hand, might be important for the top-down mechanism, since they allow consumers to compare and to balance biomasses between resource species.

Means and standard deviations of other topological properties of model food webs in the steady state are listed in Table 2 for reference. For a simple comparison with empirical data, means and standard deviations of the corresponding values obtained from a collection of 17 empirical data sets are listed as well. Of the 14 properties, the model averages of 13 are within one standard deviation of the empirical range. Model webs have a comparatively large fraction of cannibal species (Cannib), but cannibalism is known often to be underreported (Cohen et al. 1990). All 14 model averages are within two standard deviations of the empirical data. This shows that the topology of the model food webs does not exhibit any obvious artifacts that might favor the top-down mechanism. A more
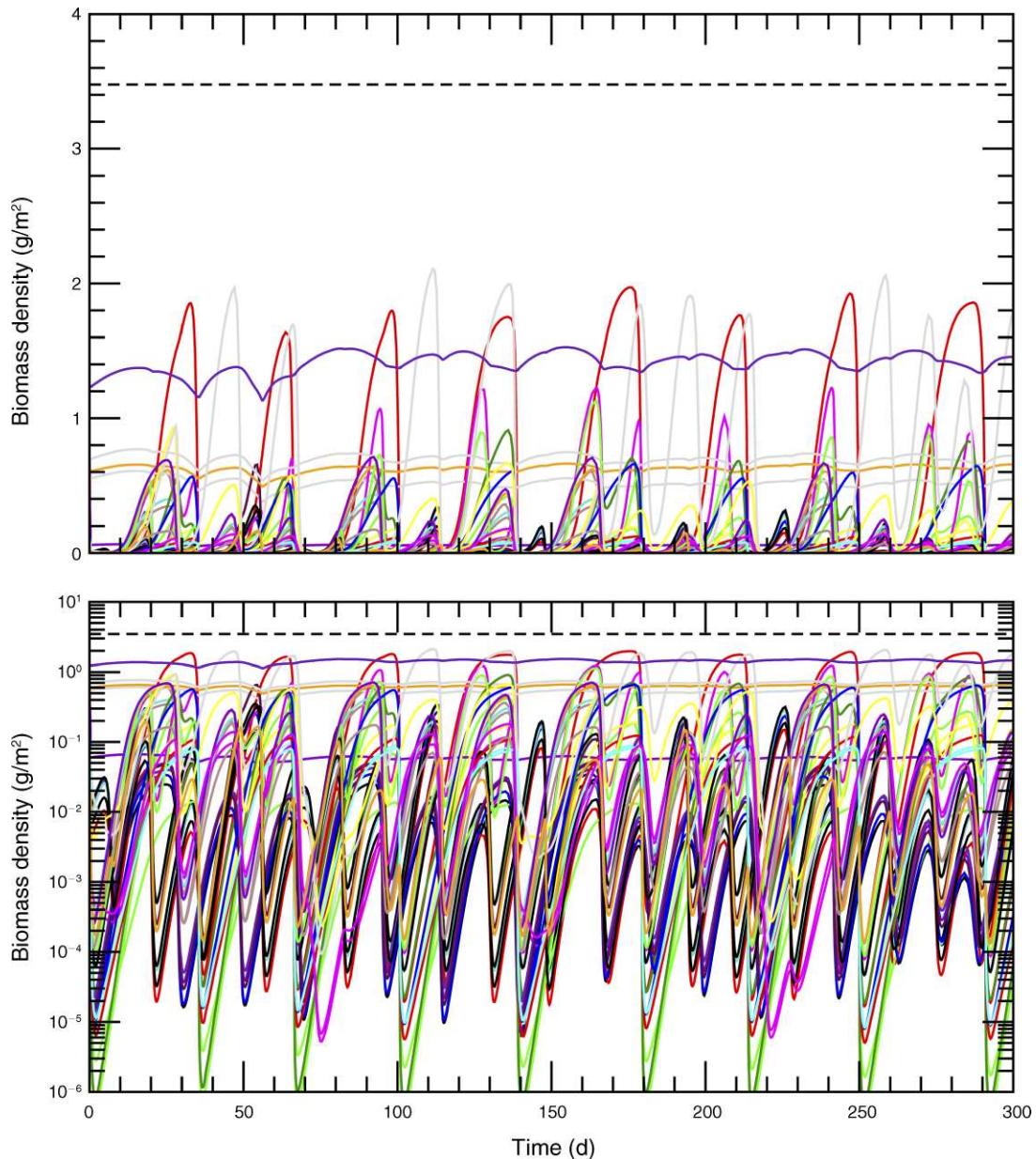
FIG. 5. Typical chaotic variations of producer (e.g., phytoplankton) biomasses in the model steady state, with parameters as given in the Appendix. Lines of different colors or gray level correspond to different species. The same data are shown on a linear scale (top) and a logarithmic scale (bottom) for comparison. The dashed horizontal line corresponds to the monoculture carrying capacity for the smallest producer species.

systematic validation of the model food web topology is desirable but beyond the purpose of the current work.

NUMERICAL EXPERIMENTS AND RESULTS

Definitions of scaling exponents

There are two different approaches commonly used for defining the scaling exponent. One is a double-logarithmic regression of the normalized size spectrum (Platt and Denman 1977, 1978), where the size spectrum is obtained by first determining the total biomasses of all

individuals in logarithmically scaled size classes and then dividing these totals by the width of the classes (which yields values of dimension abundance). The other approach is a direct double-logarithmic regression of the abundances or biomasses of all species with their mean body masses (Damuth 1981), usually taking body mass as the independent variable. The first approach is much easier to realize in field studies, in particular if the number of species is large. However, in small communities the size spectrum may have gaps with unoccupied
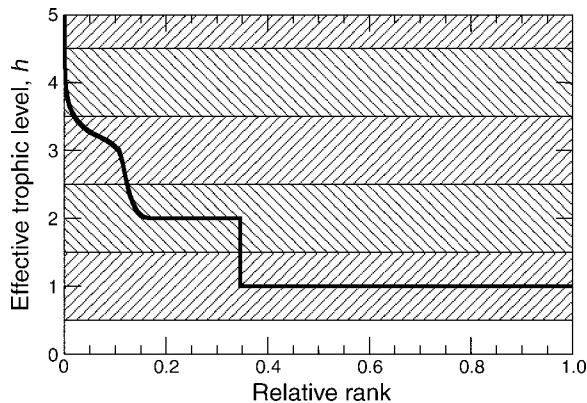
FIG. 6. The effective trophic level (*h*) of species vs. their relative rank in the steady state of the model. Producers correspond to $h = 1$. Hatching indicates the corresponding integer trophic levels obtained by rounding *h*.

FIG. 7. Typical body-mass (*M*)–abundance (*N*) relationship in a model community, with parameters as given in the Appendix. Points denote population sizes of individual species. The dashed line corresponds to a linear regression ($N \sim M^{-0.95}$). Symbols encode trophic levels, with plus signs for level 1 (producers), circles for level 2 (herbivores), squares for level 3 (carnivores), and triangles for level 4 (super carnivores). Log-transformed body mass was originally measured in kilograms, and abundance was the number of individuals.

size classes (Havlicek and Carpenter 2001), leading to singularities when taking logarithms. The second approach does not have this conceptual disadvantage, and is more robust when the number of species is small. The precise relationship between the two definitions is not clear. Results for both definitions are given in the following sections. All regressions reported are ordinary least square with $\log_{10} M$ as the independent variable.

Body mass vs. abundance scaling in simulated food webs

Direct regression.—For a typical model community, the body masses and time-averaged abundances of all species, as well as their trophic levels, are shown in Fig. 7. Direct double-logarithmic regression yields a relationship $N \sim M^{-1+\lambda}$, or $B = N \times M = M^{\lambda}$, with $\lambda = 0.05$ ($n = 79$; nominal standard error, 0.09).

When pooling the data of all saved steady-state communities of the model run with standard parameters (see the Appendix), the corresponding value is $\lambda = -0.002$ ($n = 279\,598$). When restricting the regression to
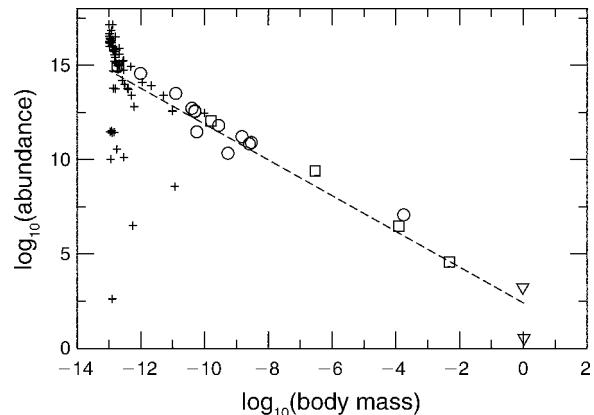
consumer species, the exponent in the relation $B \sim M^{\lambda_c}$ is $\lambda_c = 0.034$ ($n = 96\,276$). Because of strong phylogenetic and temporal correlations, which are difficult to take into account, we refrain here from computing error estimates from the underlying data. From the comparison of different simulation runs below, the standard error in λ and λ_c can be estimated as ≈ 0.02.

As we explained in *Introduction*, bottom-up theories, such as the energetic equivalence rule, predict that the scaling exponent λ in the relation $B = M \times N \sim M^{\lambda}$ is of the form $\lambda = \lambda_0 - \zeta_r$, where ζ_r is the allometric exponent for the mass-specific metabolic rates of consumers. The current model incorporates the metabolic rates of consumer species in their respiration rates and their maximum growth rates (see the Appendix).

TABLE 2. Topological properties of model food webs in the steady state (mean ± SD) at standard parameters (see the Appendix), compared to the ranges of values found in an analysis of empirical data sets.

Symbol	Simple explanation	Model	Observations
S	number of species	20 ± 8	54 ± 35
C	directed connectance	0.21 ± 0.05	0.16 ± 0.10
T	fraction of top species	0.15 ± 0.09	0.18 ± 0.19
GenSD	variability of generality	0.91 ± 0.12	1.13 ± 0.44
VulSD	variability of vulnerability	0.84 ± 0.16	0.98 ± 0.18
MxSim	trophic similarity among species	0.62 ± 0.07	0.60 ± 0.10
Cannib	fraction of cannibal species	0.37 ± 0.09	0.16 ± 0.19
aChnLg	mean food chain length	3.9 ± 1.4	6.4 ± 4.1
aChnSD	variability of chain length	1.3 ± 0.3	1.6 ± 0.7
aChnNo	$\log_{10}$(number of chains)	2.6 ± 0.8	4.3 ± 2.2
aLoop	number of loops	3 ± 3	11 ± 20
aOmniv	degree of omnivory	0.74 ± 0.13	1.0 ± 0.33
Ddiet	deviation from intervality	0.33 ± 0.20	0.22 ± 0.15
Clust	clustering coefficient	0.53 ± 0.11	0.50 ± 0.15

Note: For sources of empirical data, precise definitions of the properties, computational issues, and individual values, see Rossberg et al. (2006*a*).

To test if bottom-up theories apply to the current model, we considered a modification of the model where the allometric exponent of consumer metabolic rates ζ_r is replaced by alternative values $\zeta_r = -0.35...-0.15$. The coefficients of the corresponding scaling laws were adjusted in such a way as to keep rates constant at $M_i = 10^{-10}$ kg, near the lower end of the range occupied by consumers in the model.

This modification is a compromise between leaving as many parts of the model unchanged for better comparison with the main simulation, and consistently implementing a thought experiment to test bottom-up theories. As a result, the allometric exponents for producer physiological rates and for the background scaling of attack rates (Eq. A.11 in the Appendix), on one hand, and for consumer physiology, on the other hand, differ. But the former exponents only weakly affect the community structure. The value of the allometric exponent for producer physiological rates has little effect, since most producers have body masses near $M_{\min}$, and the effective exponent for the attack rates can be adjusted by the evolutionary mechanism.

The range of values over which ζ_r can reasonably be varied is limited. At the upper end ($\zeta_r = -0.15$) of the range investigated, the number of consumer species $S_c = 16 \pm 9$ is low, and lowering it further will destroy system-level effects resulting from the interaction of many species. At the lower end ($\zeta_r = -0.35$) the range of consumer body masses spreads out widely and is limited from above by the condition $B_i > M_i$. Reducing ζ_r further would potentially bias the B_i. Furthermore, species numbers become large ($S_c + S_p = 144$ on average) and simulations difficult. In fact, the computations for $\zeta_r = -0.35$ had to be stopped prematurely after 29 000 sa or 716 hours of simulations. But we expect that the large number of consumer species $S_c = 75 \pm 31$ in the communities for $\zeta_r = -0.35$ mostly compensates a possible losses of accuracy in λ and λ_c due to the reduced simulation time.

The simulation results displayed in Fig. 8 show no obvious relationship between λ and ζ_r or between λ_c and ζ_r. A statistical analysis confirms this impression: Linear regression yields $\lambda = -0.032(27) - 0.06(10)\ \zeta_r$ ($n = 7$, standard errors in parenthesis, residual SD $= 0.016$) and $\lambda_c = 0.036(36) + 0.14(14)\ \zeta_r$ (residual SD $= 0.021$). (Estimates and standard errors have similar values by chance.) The null hypothesis that $\lambda = \lambda_0 - \zeta_r$ with fixed λ_0 is rejected ($P = 0.0003$), the corresponding hypothesis for λ_c as well ($P = 0.0004$). Instead, the data is compatible with the null hypothesis that λ and λ_c are independent of ζ_r ($P = 0.3$ and $P = 0.4$, respectively) with means $-0.017(6)$ for λ and $0.002(8)$ for λ_c. The latter value is consistent with zero (two-sided t test, $P = 0.8$), while the former is rather not ($P = 0.025$).

Regression of size spectra.—For reasons discussed in *Definitions of scaling exponents*, scaling exponents based on size spectra become ill defined if the number of species is small. Besides, producer biomasses exhibit a
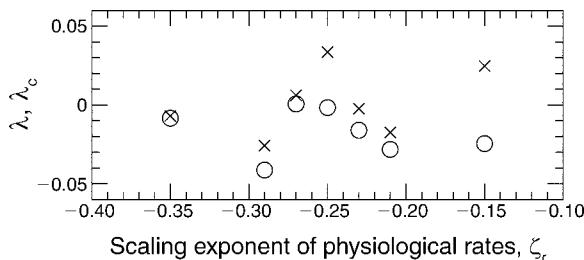

FIG. 8. Simulation results for the scaling exponent λ (population growth rate) relating biomass (B) as $B \sim M^\lambda$ to body mass M for varying allometric exponent ζ_r of consumer physiological rates (circles, λ [all species]; crosses, λ_c [consumers only]). Horizontal and vertical axis are drawn at the same scale.

larger variability than consumer biomasses (see Fig. 12), leading to non-power law size spectra if producers are included. The analysis here is therefore restricted to consumer species, and for each value of ζ_r the mean slope $\bar{v}_c$ is computed as the arithmetic mean of the slopes of the normalized size spectra of only the $n = 100$ steady-state communities with largest number of consumers S_c. Choosing $n = 50$ or $n = 200$ does not alter the statistical conclusions. Species were grouped in decimal size classes to compute the spectra. Fig. 9 displays the slopes $\bar{v}_c$ of normalized steady-state size spectra ($\zeta_r = -0.25$) vs. S_c and the $n = 100$ cutoff.

Mean slopes $\bar{v}_c$ for varying ζ_r are shown in Fig. 10. Again, there is no clear relationship. Linear regression gives $\bar{v}_c = -1.061(30) - 0.04(11)\ \zeta_r$. Here, too, the null hypothesis that $\bar{v}_c = v_0 - \zeta_r$ with fixed v_0 is rejected ($P = 0.0004$) and the hypothesis of constant $\bar{v}_c$ is accepted ($P = 0.7$). The mean value of $\bar{v}_c$ over all ζ_r is $-1.050(7)$, slightly but significantly smaller than -1 ($P = 2 \times 10^{-4}$).

If consumer abundances would scale exactly as $N \sim M^{-1+\lambda_c}$ and consumer species were distributed evenly over the M axis, a relation $v_c = -1 + \lambda_c$ would hold. The fact that simulated spectra have slightly steeper slopes is consistent with expectation, since there are more small than large species. Slopes of empirical size spectra tend to be slightly smaller than one as well (Quiñones et al. 2003).

Testing the top-down theory for body-mass–abundance scaling

Distribution of species in the body-mass–biomass plane.—In order to understand the weak dependence of λ on ζ_r, it is instructive to inspect the underlying distribution of species in the $\log(B)$–$\log(M)$ plane. Steady-state densities in the $\log(M)$–$\log(B)$ plane (Figs. 11–14) were estimated using a kernel estimator applied with equal weight to all species contained in snapshots taken over the evolutionary model steady states of all four communities every 60 sa. In order to avoid biases from the kernel, it was chosen data driven as a bivariate normal density with covariance matrix $1.5\mathbf{C} \times N^{-1/3}$, where $\mathbf{C}$ is the estimated covariance matrix of the data and N the number of sample points. The exponent $-1/3$
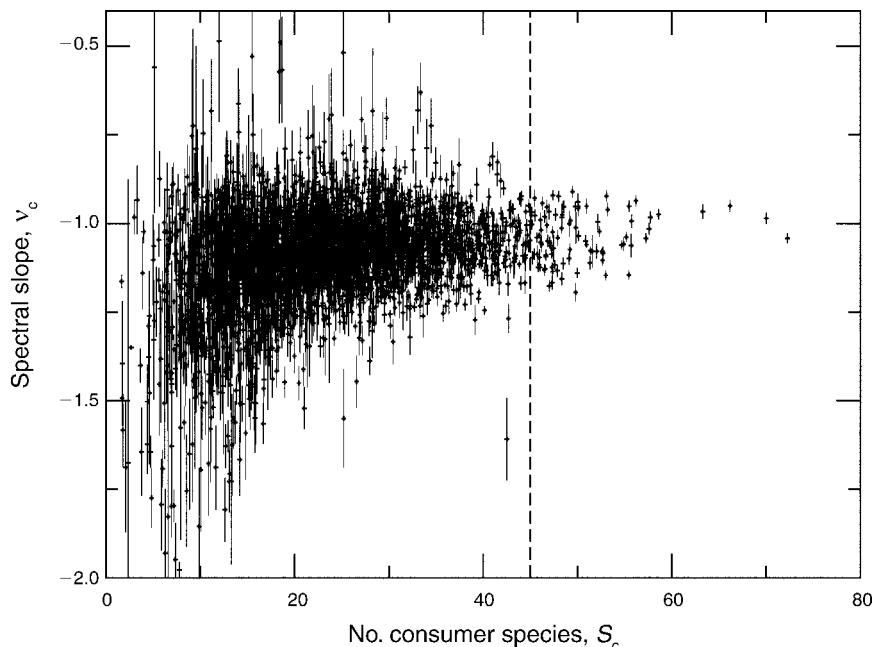
FIG. 9. Slopes of model consumer size spectra, v_c, vs. consumer species richness, S_c, with parameters as in the Appendix. Error bars indicate sample estimates of standard errors. The 100 communities to the right of the dashed line have an average slope of -1.04.

guarantees a balance between stochastic errors and errors due to smoothing for bivariate distributions.

The distribution of species in the $\log(B)$–$\log(M)$ plane is shown in Fig. 11 (standard parameters). Apparent are the region of high density at low body masses corresponding to producer species, and the long tail with roughly constant biomass stretching toward higher body masses. A more detailed picture can be obtained by splitting this distribution into the contributions from different trophic levels. This has been done in Fig. 12. The maxima of the distributions for all levels are located near a line of constant B. The positions of the maxima are listed in Table 3. The regression line through these points yields a between-level slope of -0.037. For herbivores and carnivores, the within-level slopes are also close to zero (Table 3). For super carnivores, the slope (0.144) is closer to 0.25 than to 0. However, Fig. 12 suggests that this is rather due to the extinction limit at

$B = M$ (i.e., $N = 1$) than due to the structure of the bulk of the distribution.

Communities without carnivores.—To test the hypothesis that the distribution of species in the $\log(B)$–$\log(M)$ plane is under top-down control, top-down effects were disabled in the model in two steps. First, carnivory was
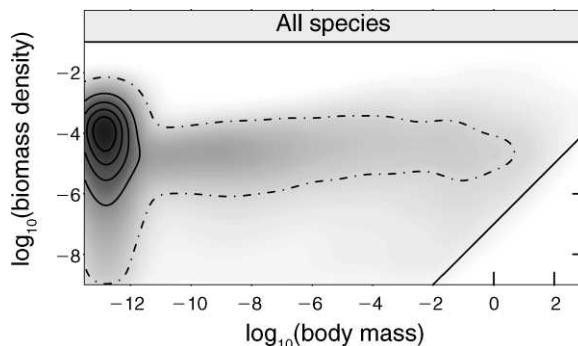

FIG. 11. Estimated density of species in the body mass–biomass plane for the model steady state, with parameters as given in the Appendix. The four solid concentric lines correspond to 80%, 60%, 40%, and 20% of the maximum density. The dash-dotted line corresponds to 2.5%. Gray levels encode intermediate densities. The solid line in the lower right corner corresponds to the extinction limit at $B = M$. The peak of the distribution at low body masses, which is dominated by producer species, is blurred by the smoothing window. With a narrower window, the long tail toward higher body masses would become invisible. For the actual density of producer species, see the top panel of Fig. 12. Body mass was originally measured in kilograms, and biomass density was measured in kilograms per square meter.
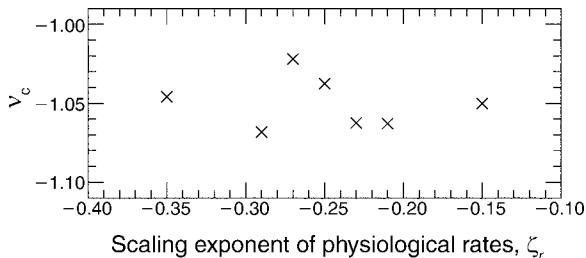

FIG. 10. Simulation results for slopes of consumer size spectra vs. the allometric exponent ζ_r of consumer physiological rates. Horizontal and vertical axes are drawn at the same scale.
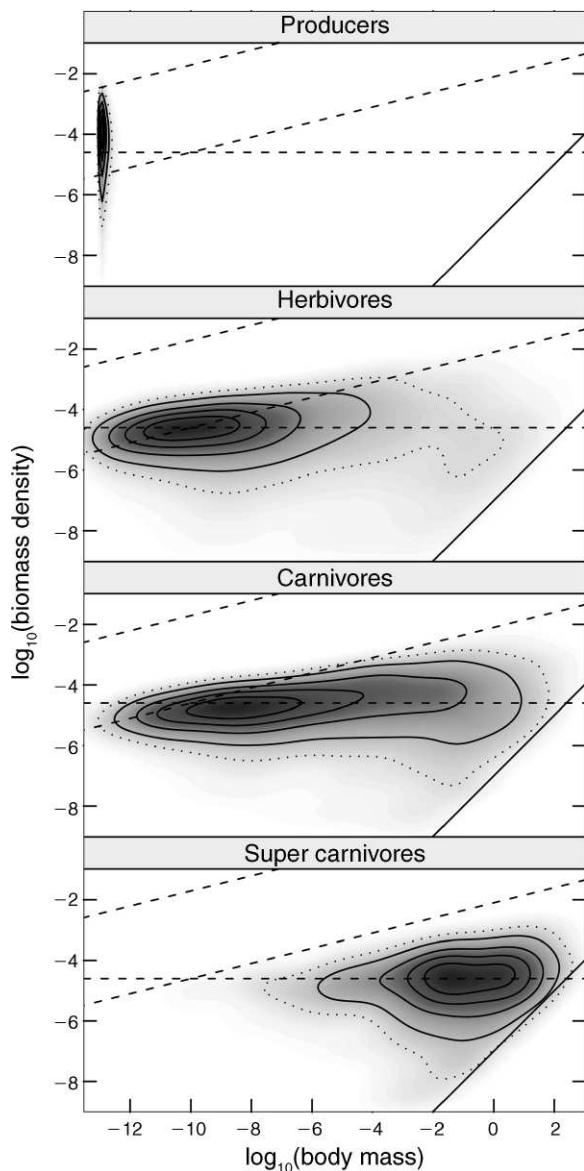
FIG. 12. Density of species in the body mass–biomass plane, separated by trophic level, in the steady state of the model, with parameters as given in the Appendix. The four solid concentric lines correspond to 80%, 60%, 40%, and 20% of the maximum density. The dotted line corresponds to 10%. Gray levels encode intermediate densities. The solid line in the lower right corner corresponds to the extinction limit at $B = M$. The dashed line in the upper left corner represents the carrying capacity for producer species in monoculture. The two other dashed lines are guides to the eye with slopes 0 and 1/4, respectively. All auxiliary lines are reproduced identically in Figs. 13 and 14. Horizontal and vertical axes are drawn at the same scale. Body mass was originally measured in kilograms, and biomass density was measured in kilograms per square meter.

TABLE 3. Characteristics of distributions displayed in Fig. 12.

	Maximum at		Slope of regression
Trophic level	$\log(M)$	$\log(B/A)$	of $\log(B)$ on $\log(M)$
Producers	−12.8	−4.0	(−2.1)
Herbivores	−10.3	−4.6	0.017
Carnivores	−8.6	−4.8	0.050
Super carnivores	−1.4	−4.6	0.144

Note: Abbreviations are: M, body mass of individuals; B, total biomass of a species; A, system area.

consumers (herbivores) and producers. Fig. 13 shows the distributions of producers and consumers in the $\log(B)$–$\log(M)$ plane for this case. The bulk of the distribution for consumers now stretches along an energetic equivalence line (slope 1/4), rather than a line of constant biomass as was the case in the full model. The numerical value obtained for the slope by ordinary least square regression is somewhat smaller (0.153), which can be attributed to the comparatively large scatter along $\log(B)$, but it is still closer to 1/4 than to zero.

Communities without consumers.—Similar observations can be also made when disabling herbivory and running the model only with producer species. Released from the need to compensate losses by grazing at the highest possible rate, larger producers can now evolve. In fact, inter-producer competition is modeled such that larger producers have a competitive advantage over smaller producers (Eqs. A.5 and A.6 in the Appendix). A large producer at its carrying capacity depletes a large part of the resources of a small producer if there is

disabled. That is, in a modification of the original model, the trophic interaction coefficients c_{ki} were set to zero whenever the resource species k was a consumer. The remaining trophic interactions were only between
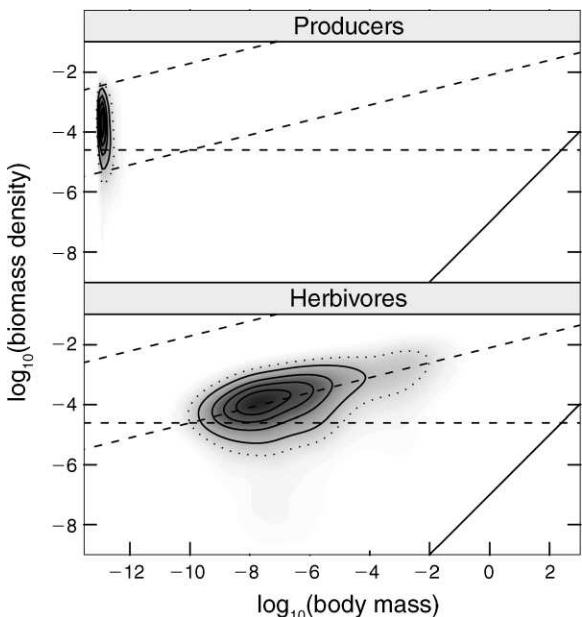

FIG. 13. Density of species in the body mass–biomass plane, separated by trophic level, for the model variant without carnivores. See Fig. 12 for details.
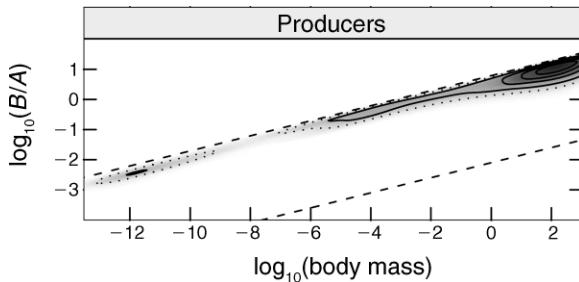
FIG. 14. Density of producers in the body mass–biomass plane (model variant without consumers). See Fig. 12 for details. Body mass was originally measured in kilograms, and B/A was in kilograms per square meter.

sufficient niche overlap, while a small producer at its carrying capacity has only a weak effect on the resources available to a large producer. As a result, producers evolve to larger sizes, limited, in this model, only by the system size or the hard upper cutoff M_{max}. Producer biomasses are close to their monoculture carrying capacities (Fig. 14, upper dashed line), in good agreement with the energetic equivalence rule.

That is, in the absence of consumption, the structure of the producer community resembles rather a forest than a planktonic community. As an aside, a similar observation can be made if, in the model, producers are allowed to evolve vulnerability traits that cannot easily be matched by the foraging traits of consumers. In the presence of consumption, trees can evolve only if equipped with a sufficiently effective defense, just as observed in nature.

The small scatter away from the energetic equivalence line in Fig. 14 might at first be surprising. It can be attributed to the simplicity of the producer sub-model. Apart from the scaling of rates and carrying capacities with body size, the population dynamics of different plant species are identical when niche overlaps are sufficiently small. The situation without carnivores (Fig. 13) is not quite as simple. Consumers differ in their attack (or grazing) rates, the degree of adaptation to, and the abundance of their resources. It is remarkable that energetic equivalence is approximately realized in these communities, too.

DISCUSSION

The results discussed above show that, in the model, (1) the body-mass–abundance scaling exponent does not change with the allometric scaling of the metabolic rates in the form predicted by bottom-up theories, (2) rather, the dependence of the exponent on the allometric scaling of the metabolic rate is weak, (3) the scaling exponent of abundance with body mass is close to −1 over a wide parameter range, which implies that the biomass of species does not depend systematically on their body mass, and (4) this scaling breaks down if top-down control is disabled. These results show that in the model the top-down mechanism is active: the biomasses of

species are in an equilibrium mediated by adaptive foraging.

Top-down control can explain why biomasses are limited from above by some equilibrium value. Together with a general heuristic argument, it can also explain why biomasses are, on a logarithmic scale, located near this equilibrium value. In order for the population of a species to saturate at some value, a mechanism for density-dependent population growth is necessary. In the model, such density-dependent mechanisms set in when a species either controls the abundance of its main resources, such that an increase of its own abundance will lead to a depletion of the resource, or when this species is the main resource for some consumer, and thus determines the abundance of the consumer and its own consumption rate. But a species that is rare compared to other, similar species will neither control the abundance of its resources, nor determine the abundance of its consumers. The population growth of a rare species does therefore not depend on its own density. On the long term, its population will either grow until it is not rare anymore, or the species will go extinct. Thus, the populations of all species are, on the log scale, near the upper limit in the population-dynamical steady state. In this context, it is worth noting that, because the dynamics of rare species is linear, the precise value of the biomass at which species invade or go extinct (here chosen as $B_i = M_i$) does not matter.

We now come back to the third question posed in the introduction and ask by which mechanism this upper limit, the equilibrium biomass, is determined. For the model, the following argument shows that this value must be determined bottom-up by the carrying capacity of producers. Since attack rates evolve freely, there are only two effects in the model that involve biomass densities as parameters: one is the extinction of rare species at $B_i = M_i$, the other is the carrying capacity of producers $B_i = K_i \sim M_i^{1/4}$ (see the Appendix). But the extinction threshold does not affect equilibrium biomasses. This is suggested by the low density of species near the line $B_i = M_i$ in Fig. 11 and the absence of such species in Fig. 13, and can be confirmed in numerical experiments varying the system size A (not shown). Producer carrying capacities are the only possible determinants of equilibrium biomass density remaining. Thus, while the biomass equilibrium is a top-down effect, the value of the equilibrium biomass density itself is controlled bottom-up.

Remarkably, time-averaged producer biomasses nevertheless remain about two orders of magnitude below their monoculture carrying capacity. We do not have a quantitative theory to predict this ratio, yet. Certainly, the strong regular or chaotic oscillations of producer biomasses (Fig. 5) are important. The maxima of these oscillations always have to remain below the carrying capacity, hence the mean values will be somewhat lower. But competition for resources between producers and consumption by herbivores will also play a role.

Taking the ratio between the monoculture carrying capacity of the smallest producers and typical mean biomasses actually reached into account by a correction factor $C \approx 100$, the equilibrium biomass is therefore give by $B = K_p/C$, where K_p is the carrying capacity for a small producer (e.g., phytoplankton) species in monoculture. The latter can be estimated as $K_p = \text{GPP}_{max}/\sigma_p$, where GPP_{max} is the gross primary production of monocultures, and σ_p is the maximum specific production rate of small producers. Thus, when the top-down mechanism is active, the prediction of the theory can be summarized by the following formula for typical abundances of species on the log scale:

$$N = \frac{\text{GPP}_{max}}{C \times \sigma_p \times M} \qquad (1)$$

where N and M are the abundance and body mass of an arbitrary species at an arbitrary trophic level. We note that, apart from C, the right-hand side of this formula contains only quantities related to the biology of individual species and the physical availability of the limiting resource, while the left-hand side describes an aspect of ecology resulting from the interaction of many species. Predicting macroecological patterns based on general biological and physical facts is perhaps the most one can expect from a general macroecological theory.

CONCLUSIONS

Based on simulation results using a general multi-trophic community model, we conclude that the top-down mechanism is a viable alternative to bottom-up mechanisms in controlling body-mass–abundance scaling. The top-down mechanism naturally leads to biomass densities independent of body mass, as they are frequently observed.

Since, in the model, the top-down mechanism operates at least partially on the evolutionary time scale, it might be difficult to identify it in the field. On population-dynamical time scales, one might simply find ecological parameters "magically" adjusted such as to yield constant biomass across trophic levels under bottom-up control. More research is necessary to better understanding the relative importance of evolutionary and population-dynamical contributions to the top-down mechanism.

Just as constant biomass is not always observed in nature, and many communities do show patterns compatible with the simple energetic equivalence rule, our model did not yield constant biomass for every parameter set considered. If, for example, parameters were chosen such that no or only few carnivores could evolve, we often observed a biomass dominance of large herbivores. We would therefore caution to conclude that the top-down mechanism is active in nature under all circumstances. But we believe that, in view of the ongoing debate and the unresolved issues surrounding body-mass–abundance scaling, the idea deserves more attention.

LITERATURE CITED

Amaral, L. A. N., and M. Meyer. 1999. Environmental changes, coextinction, and patterns in the fossil record. Physical Review Letters 82(3):652–655.

Banašek-Richter, C., M.-F. Cattin, and L.-F. Bersier. 2005. Food web structure: from scale invariance to scale dependence and back again? Pages 48–55 in P. de Ruiter, V. Wolters, and J. C. Moore, editors. Dynamic food webs. Academic Press, Amsterdam, The Netherlands.

Benoît, E., and M.-J. Rochet. 2004. A continuous model of biomass size spectra governed by predation and the effects of fishing on them. Journal of Theoretical Biology 226(1):9–21.

Bersier, L.-F., and P. Kehrli. 2008. The signature of phylogenetic constraints on food-web structure. Ecological Complexity, in press.

Blackburn, T., and K. Gaston. 1999. The relationship between animal abundance and body size: a review of mechanisms. Advances in Ecological Research 28:181–210.

Brose, U., et al. 2006. Consumer–resource body-size relationships in natural food webs. Ecology 87:2411–2417.

Brown, J. H., J. F. Gillooly, A. P. Allen, V. M. Savage, and G. B. West. 2004. Toward a metabolic theory of ecology. Ecology 85:1771–1789.

Caldarelli, G., P. G. Higgs, and A. J. McKane. 1998. Modelling coevolution in multispecies communities. Journal of Theoretical Biology 193:345.

Carbone, C., and J. L. Gittleman. 2002. A common rule for the scaling of carnivore density. Science 295:2273–2276.

Christian, R. R., and J. J. Luczkovich. 1999. Organizing and understanding a winter's seagrass foodweb network through effective trophic levels. Ecological Modelling 117:99–124.

Claessen, D., C. van Oss, A. M. Roos, and L. Persson. 2002. The impact of size-dependent predation on population dynamics and individual life history. Ecology 83:1660–1675.

Cohen, J. E., F. Briand, and C. M. Newman. 1990. Community food webs: data and theory. Volume 20 of Biomathematics. Springer, Berlin, Germany.

Cohen, J. E., T. Jonsson, and S. R. Carpenter. 2003. Ecological community description using the food web, species abundance, and body size. Proceedings of the National Academy of Science (USA) 100:1781–1786.

Currie, D. J. 1993. What shape is the relationship between body size and population density? Oikos 66:353–358.

Cyr, H. 2000. The allometry of population density and interannual variability. Pages 267–295 in J. H. Brown and G. B. West, editors. Scaling in biology. Oxford University Press, Oxford, UK.

Damuth, J. 1981. Population density and body size in mammals. Nature 290:699–700.

Damuth, J. 2007. A macroecological explanation for energy equivalence in the scaling of body size and population density. American Naturalist 169(5):621–631.

Drossel, B., P. G. Higgs, and A. J. McKane. 2001. The influence of predator–prey population dynamics on the long-term evolution of food web structure. Journal of Theoretical Biology 208:91–107.

Drossel, B., A. J. McKane, and C. Quince. 2004. The impact of nonlinear functional responses on the long-term evolution of food web structure. Journal of Theoretical Biology 229:539–548.

Duarte, C. M., S. Agusti, and H. Peters. 1987. An upper limit to the abundance of aquatic organisms. Oecologia 74(2):272–276.

Dunne, J. A., R. J. Williams, N. D. Martinez, and R. Tiburon. 2002. Network structure and biodiversity loss in food webs: robustness increases with connectance. Ecology Letters 5:558–567.

Gaedke, U. 1992. The size distribution of plankton biomass in a large lake and its seasonal variability. Limnology and Oceanography 37(6):1202–1220.

Greenwood, J. J. D., and R. A. Elton. 1979. Analysing experiments on frequency-dependent selection by predators. Journal of Animal Ecology 48:721–737.

Griffiths, D. 1992. Size, abundance, and energy use in communities. Journal of Animal Ecology 61:307–315.

Havlicek, T., and S. R. Carpenter. 2001. Pelagic species size distributions in lakes: are they discontinuous? Limnology and Oceanography 46:1021–1033.

Jeschke, J. M., M. Kopp, and R. Tollrian. 2004. Consumer-food systems: why type I functional responses are exclusive to filter feeders. Biological Reviews 79:337–349.

Jonsson, T., J. E. Cohen, and S. R. Carpenter. 2005. Food webs, body size, and species abundance in ecological community description. Advances in Ecological Research 36:1–84.

Levine, S. 1980. Several measures of trophic structure applied to complex food webs. Journal of Theoretical Biology 83:195–207.

Li, B.-L., V. G. Gorshkov, and A. M. Makarieva. 2004. Energy partitioning between different-sized organisms and ecosystem stability. Ecology 85:1811–1813.

Loeuille, N., and M. Loreau. 2005. Evolutionary emergence of size-structured food webs. Proceedings of the National Academy of Science (USA) 102(16):5761–5766.

Loeuille, N., and M. Loreau. 2006. Evolution of body size in food webs: does the energetic equivalence rule hold? Ecology Letters 9:171–178.

Marquet, P. A. 2002. Of predators, prey, and power laws. Science 295:2229–2230.

Marquet, P. A., S. A. Navarrete, and J. C. Castilla. 1995. Body size, population density, and the energetic equivalence rule. Journal of Animal Ecology 64:325–332.

Marquet, P. A., R. A. Quiñones, S. Abades, F. Labra, and M. Tognell. 2005. Scaling and power-laws in ecological systems. Journal of Experimental Biology 208:1749–1769.

May, R. M. 1972. Will a large complex system be stable? Nature 238:413–414.

McNiel, S., and J. H. Lawton. 1970. Annual production and respiration in animal populations. Nature 225:472–474.

Meehan, T. D. 2006. Energy use and animal abundance in litter and soil communities. Ecology 87:1650–1658.

Mulder, C., J. E. Cohen, H. Setälä, J. Bloem, and A. M. Breure. 2005. Bacterial traits, organism mass, and numerical abundance in the detrital soil food web of Dutch agricultural grasslands. Ecology Letters 8:80–90.

Nee, S., A. F. Read, J. Greenwood, and P. Harvey. 1991. The relationship between abundance and body size in British birds. Nature 351:312–313.

Oaten, A., and W. Murdoch. 1975. Switching, functional response, and stability in predator–prey systems. American Naturalist 109(967):299–318.

Peters, R. H. 1983. The ecological implications of body size. Cambridge University Press, Cambridge, UK.

Platt, T., and K. Denman. 1977. Organization in the pelagic ecosystem. Helgolander Wissenschaftliche Meeresuntersuchungen 30:575–581.

Platt, T., and K. Denman. 1978. The structure of pelagic ecosystems. Rapports et Procès-Verbaux des Réunions du Conseil International pour l'Exploration de la Mer 173:60–65.

Quiñones, R. A., T. Platt, and J. Rodríguez. 2003. Patterns of biomass–size spectra from oligotrophic waters of the Northwest Atlantic. Progress in Oceanography 57:405–427.

Rodriguez, J., and M. Mullin. 1986. Relation between biomass and body weight of plankton in a steady state oceanic ecosystem. Limnology and Oceanography 31:361–370.

Rossberg, A. G. 2008. Part-whole relations between food webs and the validity of local food-web descriptions. Ecological Complexity, in press.

Rossberg, A. G., H. Matsuda, T. Amemiya, and K. Itoh. 2006a. Food webs: experts consuming families of experts. Journal of Theoretical Biology 241(3):552–563.

Rossberg, A. G., K. Yanagi, T. Amemiya, and K. Itoh. 2006b. Estimating trophic link density from quantitative but incomplete diet data. Journal of Theoretical Biology 243(2):261–272.

Savage, V. M., J. F. Gillooly, J. H. Brown, G. B. West, and E. L. Charnov. 2004. Effects of body size and temperature on population growth. American Naturalist 163(3):429–441.

Sheldon, R. W., A. Prakash, and W. H. Sutcliffe. 1972. The size distribution of particles in the ocean. Limnology and Oceanography 17:327–340.

Solé, R. V., S. C. Manrubia, M. Benton, and P. Bak. 1997. Self-similarity of extinction statistics in the fossil record. Nature 388:764–767.

Sprules, W. G., and M. Munawar. 1986. Plankton size spectra in relation to ecosystem productivity, size, and perturbation. Canadian Journal of Fisheries and Aquatic Science 43:1789–1794.

Whittaker, R. H. 1965. Dominance and diversity in plant communities. Science 147:250–260.

Williams, R. J., and N. D. Martinez. 2000. Simple rules yield complex food webs. Nature 404:180–183.

Yoshida, K. 2003. Dynamics of evolutionary patterns of clades in a food web system model. Ecological Research 18:625–637.

APPENDIX

Model details (*Ecological Archives* E089-031-A1).

DATA REGISTRY

The C++ simulation code and sample data generated by the model are registered (ESA Data Registry esa.45.1).

The top-down mechanism for body mass – abundance scaling

A. G. Rossberg, R. Ishii, T. Amemiya, K. Itoh

Appendix A: Model Details

In the following, we give a compact technical definition of the full model, suitable for writing a numerical simulation code. The parametrization and the motivations and implications of design decisions are discussed in Section A2. Table A1 lists model parameters and variables.

A1 Model Definition

A1.1 Model states

Each consumer species i is characterized by its mean body mass M_i ($M_{\min} \leq M_i \leq M_{\max}$), its current total biomass $B_i(t)$, a D-dimensional vector of abstract quantitative vulnerability traits $\vec{V}_i$, another D dimensional vector $\vec{F}_i$ describing foraging traits and capabilities, its attack rate a_i, and a switching exponent b_i. Producer species i are characterized by M_i, $B_i(t)$, $\vec{V}_i$, and a D-dimensional vector $\vec{G}_i$ describing the non-trophic producer niche.

A community is fully characterized by its constituent consumers and producers. The complete model state consists of four communities.

A1.2 Population dynamics

Consumer population dynamics is of the standard form

$$\frac{dB_i}{dt} = \epsilon \overbrace{\sum_{\text{species k}} f_{ki} B_i}^{\text{eating}} - \overbrace{\sum_{\text{consumers } l} f_{il} B_l}^{\text{being eaten}} - \overbrace{r_i B_i}^{\text{respiration}} \quad . \tag{A.1}$$

The the functional response f_{ki} has been constructed in such a way as to satisfy three conditions. If there is only a single resource species or if all resource abundances are scaled by the same factor, the standard Type II form should be recovered, because Type II responses are overwhelmingly observed (Jeschke et al., 2004). If, on the other hand, resource abundances vary disproportionally, the relative intake should follow the power-law form $f_{ki}/f_{li} \sim (B_k/B_l)^{b_i}$ which is found in experiments (e.g., Greenwood and Elton, 1979; Elliott, 2004). Finally the biomasses of species not contributing to the diet should not affect the functional response. These conditions are satisfied by

$$f_{ki} = \frac{a_i \left(c_{ki} B_k\right)^{b_i}}{\beta_i^{b_i-1} + T_i a_i \sum_j (c_{ji} B_j)^{b_i}} \text{ with } \log \beta_i = \frac{\sum_j c_{ji} B_j \log c_{ji} B_j}{\sum_j c_{ji} B_j}, \tag{A.2}$$

with a_i and T_i representing the attack rate and the "handling time" of consumer i, and the c_{ki} denoting trophic interaction coefficients.

However, this form fails to satisfy a "common sense" condition pointed out by Arditi and Michalski (1995) and Berryman et al. (1995): Dynamics is not invariant if a resource population is formally split into two populations with identical traits.

This problem can be overcome by organizing resources k into groups $\gamma = \Gamma(k)$ of similar species, within which consumers cannot distinguish when switching prey. Among group members,

consumers forage proportional to the resource availability $c_{ki}B_k$. The groups are formed, for simplicity, by dividing the D-dimensional trophic niche space into a lattice of cells with lattice constant u, and assigning all species with a vulnerability $\vec{V}_k$ in the same cell to the same group. Denote by $A_{\gamma i} = \sum_{\Gamma(k)=\gamma} c_{ki}B_k$ the total availability of resource species in group γ to consumer i. Then, a second, "common sense", form of the functional response is given by

$$f_{ki} = \frac{c_{ki}B_k}{A_{\Gamma(k)i}} \cdot \frac{a_i\, A_{\Gamma(k)i}^{b_i}}{\beta_i^{b_i-1} + T_i a_i \sum_\gamma A_{\gamma i}^{b_i}} \text{ with } \log \beta_i = \frac{\sum_\gamma A_{\gamma i} \log A_{\gamma i}}{\sum_\gamma A_{\gamma i}}. \tag{A.3}$$

When no two $\vec{V}_k$ are identical, which is practically always the case with the evolutionary dynamics given below, the second from of the functional response goes over into the first form (A.2) in the limit of small cells $u \to 0$.

The trophic interaction coefficients are composed as

$$c_{ki} = \overbrace{\exp\left[-\frac{|\vec{V}_k - \vec{F}_i|^2}{2\,w_t^2}\right]}^{\text{trophic trait matching}} \times \overbrace{\left(\frac{M_k}{M_i}\right)^\alpha}^{\text{small resource cutoff}} \times \begin{cases} \overbrace{\exp(-\Lambda\, M_k/M_i)}^{\text{large resource cutoff}} & \text{for consumer } k, \\ 1 & \text{for producer } k, \end{cases} \tag{A.4}$$

where the form of the last two factors follows Claessen et al. (2002).

Producer population dynamics is modeled as

$$\frac{dB_i}{dt} = \sigma_i \overbrace{\exp\Big(-\underbrace{\sum d_{ij}B_j}_{\text{producers } j}\Big)B_i}^{\text{competition, resource exploitation}} - \overbrace{\underbrace{\sum f_{ik}B_k}_{\text{consumers } k}}^{\text{being eaten}} - \overbrace{l_i B_i}^{\text{losses}}, \tag{A.5}$$

The exponential form of the factor describing the availability of resources in the first term is inspired by the attenuation of light (Monsi and Saeki, 1953), but it could describe the depletion of other resources as well.

The matrix d_{ij} describes producer competition and self-interaction. Mutualistic and parasitic producer-producer interactions are not included in the model. The niche overlap between two producer species i, j is modeled as $\exp[-|\vec{G}_i - \vec{G}_j|^2/2w_r^2]$, with w_r denoting the producer niche width. This leads to the resource competition matrix

$$d_{ij} = d_{jj} \overbrace{\exp\left[-\frac{|\vec{G}_i - \vec{G}_j|^2}{2\,w_r^2}\right]}^{\text{producer niche overlap}}. \tag{A.6}$$

The species-specific coefficients follow allometric scaling laws $d_{jj}, l_j \sim M_j^\zeta$ and $r_j, T_j^{-1} \sim M_j^{\zeta_r}$, with $\zeta = \zeta_r = -1/4$ in the standard case.

A1.3 Species evolution

Next, we describe the implementations of "speciations" and "invasions" in the model. As explained in Sec. 2.2 of the main text, these are extremely coarse-grained descriptions of the actual evolutionary processes. To model a "speciation", the properties of a descendant species j are obtained by mutating the properties of its ancestor i. The biomass of the descendant species is given by

$$M_j = d^\xi M_i \tag{A.7}$$

with ξ denoting a standard-normal random variable, newly sampled at each use. If M_j falls outsize the range $[M_{\min}, M_{\max}]$, it is projected back into this range by the operations $M_j \to M_{\min}^2/M_j$ or $M_j \to M_{\max}^2/M_j$, which correspond to simple reflections on the log scale (Rossberg et al., 2006). Traits mutate as

$$\vec{V}_j = \frac{\left(\vec{V}_i - \vec{V}_j^0\right) + \mu_V \vec{\xi}}{\sqrt{1 + \mu_V^2/\sigma_V^2}} + \vec{V}_j^0, \tag{A.8}$$

$$\vec{F}_j = \frac{\vec{F}_i + \mu_F \vec{\xi}}{\sqrt{1 + \mu_F^2/\sigma_F^2}}, \tag{A.9}$$

$$\vec{G}_j = \frac{\vec{G}_i + \mu_G \vec{\xi}}{\sqrt{1 + \mu_G^2/\sigma_G^2}}, \tag{A.10}$$

with $\vec{V}_j^0 = (s_j, 0, 0, 0, 0)$, $s_j = s/2$ for producers and $s_j = -s/2$ for consumers, to model the distinct characteristics of the members of the two kingdoms as resources. The $\vec{\xi}$ denote standard normal random vectors, the μs and σs are model parameters.

The attack rate of the descendant species is given by

$$a_j = \left(\frac{M_j}{M_i}\right)^\zeta \times a_0 \times \tilde{a}_0^\xi \times a_i \tag{A.11}$$

This inheritance rule has the following interpretation: The first factor implies a background allometric scaling of attack rates with body mass, $a_i \sim M_i^\zeta$, the second factor, with $0 < a_0 < 1$, describes a degeneration of aggressivity in the absence of evolutionary pressures, and the third factor contributes a random mutation. Equation (A.11) is set up to be scale free in the sense that it does not imply a typical order of magnitude for the attack rates a_i or the allometric coefficients $a_i (M_i/M_0)^{-\zeta}$. This follows from the fact that all three parameters ζ, a_0, $\tilde{a}_0$ in Eq. (A.11) are dimensionless, while the a_i have dimensions of $(\text{time} \times \text{biomass})^{-1}$.

The heredity of switching exponents is assumed to be negligibly small. Thus b_j is simply given by

$$b_j = b_0 + \tilde{b}_0 \xi \tag{A.12}$$

with constant b_0 and $\tilde{b}_0$.

Except for the attack rates, this model of speciation implies a simple neutral theory: In the steady-state distribution resulting from speciations as above and random extinctions, log body masses are distributed uniformly in $[\log M_{\min}, \log M_{\max}]$, and trait vectors are given by

$$\vec{V}_i = \sigma_V \vec{\xi} + \vec{V}_i^0, \quad \vec{F}_i = \sigma_F \vec{\xi}, \quad \vec{G}_i = \sigma_G \vec{\xi}. \tag{A.13}$$

To model the "invasion" of species, two pools of representative species are assembled from the other three communities as described below, one for producers and one for consumers. The

3

properties of an invading species are obtained by picking one species from the pool at random, and mutating it in the same way as for speciations. The additional mutation represents evolutionary changes occurring in the surrounding, not explicitly modeled, communities (Fig. 1).

If a species pool is empty, which happens only in the initial phase of the simulation with the parameters used here, an invading species is sampled from the steady state of the neutral theory, with the attack rate set to $a_i = a_{\text{start}}(M_i/M_0)^\zeta$ with constant a_{start}.

Initial biomasses B_j of speciating or invading species are set to M_j.

A1.4 Community evolution

The community evolves by repeated additions (successful speciations or invasions) of a producer and a consumers species and the subsequent relaxations to the population-dynamical steady state. If a species reaches $B_i < M_i$ during the relaxation, it is removed as extinct. A speciation or invasion is successful (and hence an addition) if its population initially grows ($dB/dt > 0$). Speciation and invasions are repeatedly attempted until successful[3]. At each repetition, the attempted addition is an invasion with probability $\kappa/(\kappa + S_p)$, were S_p denotes the producer species abundance, and otherwise a speciation from a producer species chosen randomly form the local community. Correspondingly for additions of consumers.

Simulations are initiated with four empty communities and run until an evolutionary steady state is reached.

A1.5 Construction of representative species pools

Representative species pools for invasions of communities by producers are constructed by combining all producer species from the other three modeled communities, and correspondingly for consumers. To reduce waiting times when parallelizing the simulations, the information about the species compositions of the other communities is updated only after every 30 additions of one consumer and one producer, i.e., a total of 60 s.a., into each of the four communities.

A1.6 Numerical implementation

With body masses spanning 12 to 14 orders of magnitudes, and the corresponding time scales spanning tree to four, special care was required with the numerical implementation of the population-dynamical sub-model. For a stable, accurate, and fast numerical integration, the population-dynamic equations (A.1) and (A.5) were first transformed to new dependent variables $\hat{B}(t) = \ln B(t)$, and then integrated using the adaptive-order, adaptive-stepsize, implicit ODE solver CVODE included in the SUNDIALS package (Hindmarsh et al., 2005).

In order to approach the population-dynamical steady state, simulations were continued until either limit-cycle oscillations or chaotic oscillations were detected using heuristic algorithms, or until a long time T_{SS} had passed without detecting either, which usually indicates the vicinity of a fixed point. As mentioned above, species i with $B_i < M_i$ were removed as locally extinct during simulations.

---

[3]In about 2% of all cases, no species with positive growth rate can be found for a given population-dynamical state, even after 1000 attempts. In order to avoid blocking the simulations, the condition $dB/dt > 0$ is then dropped, and the addition is counted as "successful", even though the inserted species will immediately go extinct.

The four communities were simulated on separate processors. After every 60 s.a. in each community and the subsequent population-dynamical relaxation to the steady state, the full model state was saved for an update of species pools among communities (see Sec. A1.5) and for later data analysis.

A2   Model design and parameter choices

In this Appendix, the rational behind several aspects of model design and parameter choices is explained. It begins with a discussion of two aspects of niche-space structure: phylogenetic correlations of trophic traits and the number of dimensions of the niche space. Then, the parametrization and allometry of consumer and producer population dynamics is derived from empirical data; followed by a brief account of the parametrization of other aspects of trophic interaction. For some aspects of the model, most of them related to the geometry of niche space, satisfactory empirical data do not seem to be available. These have been adjusted "by hand" following the criteria discussed at the end of this Appendix.

A2.1   Phylogenetic correlations

The staring point for constructing the present model was the matching model (Rossberg et al., 2006). In the matching model, food webs are constructed by a branching process that models the evolution of the member species. It is a neutral theory, in the sense that evolution is undirected, independent of the fitness or population dynamics of species. Trophic links are determined by matching abstract traits determining the vulnerabilities of potential resources to consumption with abstract traits determining the foraging capabilities and strategies of consumers.

Fitting the matching model to empirical data, Rossberg et al. (2006) found that the heredity of vulnerability traits in local "speciations" (*sensu* Sec. 2.2) is considerably larger than of foraging traits: the median (average) of the decay rate of correlations in the vulnerability traits over all predatory food webs investigated is 1.4% per "speciation" (1.8%), while correlations between foraging traits decay by 22% per "speciation" (36%). This observation was interpreted as indicating that the evolutionary pressure through competition for resources is stronger than the pressure through indirect competition due to common predators. L.-F. Bersier (priv. comm.) suggested an alternative interpretation, which is employed in the present model: Foraging traits are simply more easily adjustable than vulnerability traits, and have higher variability.

In the neural theory for the present model, the correlation-decay rate of vulnerability traits $\vec{V}_i$ is $1 - (1 + \mu_V^2/\sigma_V^2)^{-1/2} \approx \mu_V^2/2\sigma_V^2$ per speciation, where μ_V is the magnitude of typical mutations in speciations, and σ_V is the steady-state variability of traits. (Similar results hold for foraging traits $\vec{F}_i$ and producer-interaction traits $\vec{G}_i$.) However, in the presence of evolutionary pressures, both the magnitude of mutations and the steady-state variability for the $\vec{V}_i$ will increase, and the variability of foraging traits is restricted to the variability of the corresponding vulnerability traits, and all these quantities are difficult to predict in advance. Thus, reproducing the observed patterns of trait correlations quantitatively is not easy. Yet, in order to stay in line with observations, parameters were chosen such as to keep the decay of correlations of foraging traits large, $(\mu_F/\sigma_F)^2 = \mathcal{O}(1)$, and the decay of correlations of vulnerability traits small, $(\mu_F/\sigma_F)^2 = \mathcal{O}(1\%)$. Regarding the correlations of $\vec{G}_i$ in speciations, no empirical data could be obtained.

A2.2 Dimensionality of niche space

For the matching model, it has been argued that the dimensionality of the trophic niche space does not matter much, as long as it is not too small (Rossberg et al., 2006). An important effect of high dimensionality D, i.e., of many relevant traits, is that different consumers are likely to consume the same resources for different reasons (Rossberg, 2007): Consider the situation that two consumers 1 and 2 have foraging traits $\vec{F}_1$ and $\vec{F}_2$ that are both close to the vulnerability traits $\vec{V}_3$ of resource 3, such that the factor $e_{ki} := \exp(-|\vec{V}_k - \vec{F}_i|^2/2w_t^2)$ entering the interaction coefficients Eq. (A.4) is comparatively large (an exact match is very unlikely). Then, if $\vec{F}_1$ is also close to another, unrelated $\vec{V}_4$, this does not imply that $\vec{F}_2$ is likely to be close to $\vec{V}_4$, too, if the number of dimensions is large. This is because then $\vec{F}_1$ and $\vec{F}_2$ are likely to approach $\vec{V}_3$ from different directions. Mathematically, the relevant quantity is the correlation ρ_D between the two products $e_{3,1} \times e_{3,2}$ and $e_{4,1} \times e_{4,2}$. When evaluating this correlation numerically, for example, with independent, D-dimensional, multivariate standard normal $\vec{F}_1$, $\vec{F}_2$, $\vec{V}_3$, and $\vec{V}_4$ and the niche width $w_t = 0.446$ (Tab. A1), one obtains $\rho_1 = 0.25$, $\rho_2 = 0.16$, $\rho_3 = 0.096$, $\rho_4 = 0.055$, and $\rho_5 = 0.030$. The correlations decay exponentially, roughly by a factor 0.6 with each additional dimension.

We find that the standard error in estimating ρ_5 from N independent quadruples of samples is approximately $\rho_5 \times 150\,N^{-1/2}$, that is, detecting that $\rho_5 \neq 0$ requires about $(2 \times 150)^2 = 90000$ independent quadruples. Since typical model food webs consist only of ~ 100 species, and these are phylogenetically correlated, it is fair to assume that when choosing $D = 5$ the phylogenetic correlation structure underlying food-web topology is hardly distinguishable from that with any larger number of dimensions in the model. Here, $D = 5$ is used. With an even larger number of dimensions, the volume of the accessible niche space, which scales as the variability of vulnerability traits to the Dth power, and, as a result, the number of species, would be difficult to control.[4]

A2.3 Consumer physiology

Consumer population dynamics is characterized by the gross conversion efficiency ϵ, respiration rates r_i, "handing times" T_k, attack rates a_k, and the trophic interaction coefficients.

To determine the first three parameters, consider a situation of abundant resources (*ad libitum* feeding) for species i. Then, for both forms of the functional response (A.2), (A.3), the summed functional response reduce to $\sum_l f_{li} = 1/T_i$ and, in the absence of predation, population i increases at its maximal growth rate $r_{\max,i} = \epsilon/T_i - r_i$.

While producing biomass at a rate $P = (\epsilon/T_i - r_i)B_i$, species i is, by the passive consumption terms of Eqs. (A.1) and (A.5) summed over all resource species, consuming biomass at a rate B_i/T_i. Thus, the net conversion efficiency is $\epsilon_0 = \epsilon - r_i T_i$. We set $\epsilon_0 = 0.2$, a typical empirical value for poikilotherms (Peters, 1983).

The term $-r_i B_i$ in Eq. (A.1) represents all losses other than by passive consumption. Usually, this will be dominated by respiration, losses by natural death are negligibly small.[5] Observed values for the ratio P/R of production to respiration vary from ~ 10 or higher for bacteria to ~ 0.01 for homeotherms (McNiel and Lawton, 1970). We use the value found by McNiel and Lawton for "short-lived poikilotherms", $P/R = 0.8$. Altogether, these considerations lead to

---

[4]For the neutral matching model (Rossberg et al., 2006) a much higher number of traits is used in order to reduce discretization effects, since, contrary to the situation here, the matched traits are binary (yes/no). The number of species in this model does not depend on niche-space geometry.

[5]Since the model does not describe birth or death of individuals, effects of demographic stochasticity are not included. They would have little effect on the results, since most populations are large (Fig. 12).

$$\epsilon = \left(1 + \frac{R}{P}\right)\epsilon_0, \quad T_i = \frac{\epsilon_0}{r_{\text{max},i}}, \quad r_i = \frac{R}{P} r_{\text{max},i}. \tag{A.14}$$

The maximum consumer population growth rate $r_{\text{max},i}$ is known to follow an allometric scaling law. Based on the result of Savage et al. (2004) for intermediate temperatures, we set $r_{\text{max},i} = 0.81 \,\text{yr}^{-1} (M_i/M_0)^{\zeta_r}$, with $\zeta_r = -1/4$.

In correspondence with the range of switching exponents obtained by Greenwood and Elton (1979) in a re-analysis of 14 laboratory experiments, we set the mean switching exponent to $b_0 = 1.5$ and its standard deviation to $\tilde{b}_0 = 0.3$. Field data on prey switching still seem to be rare (Elliott, 2004).

A2.4 Producer physiology and interaction

The model for producer population dynamics Eq. (A.5) implies a maximal population growth rate for producers $\sigma_{\text{max},i} = \sigma_i - l_i$, which is set to $\sigma_{\text{max},i} = \sigma_{\text{max},0} (M_i/M_0)^{-1/4}$ with $\sigma_{\text{max},0} = 0.208 \,\text{year}^{-1}$ after Niklas and Enquist (2001). The ratio between the maximum growth rate $\sigma_i - l_i$ and the respiration rate l_i was set to $(\sigma_i - l_i)/l_i = (1 - 0.1)/0.1 = 9$ as a plausible value.[6]

To determine the diagonal elements of the resource competition matrix d_{ij}, Eq. (A.6), we make use of the fact that the maximal production of producers at their carrying capacity $B_i = K_i$ is uncorrelated to their body mass (Enquist et al., 1998). Therefore, carrying capacities are chosen such that the maximal gross primary production defined by $\text{GPP}_{\text{max}} = \sigma_i K_i$ is constant. (Since the losses described by the factors l_i include both respiration and litter fall, the model does not define the net primary production.) As a convention, GPP_{max} and the K_i are here understood as extensive quantities, that it, they are proportional to the area A covered by each of the modeled communities. By Eq. (A.5), the carrying capacity of monocultures of producers is $K_i = (1/d_{ii}) \log(\sigma_i/l_i)$, which, in turn, determines the diagonal elements of the competition matrix as

$$d_{ii} = \sigma_i \frac{\log(\sigma_i/l_i)}{\text{GPP}_{\text{max}}}. \tag{A.15}$$

A2.5 Other aspects of trophic interaction

Prey switching facilitates coexistence in the model, especially between producers. In particular, we found that with the first form for the functional response, or the second form with $u \to 0$, which imply switching between any pair of resources, communities sometimes fall into unrealistic "gardening" states where a few tens of herbivores mediate coexistence of thousands of producers. With our choice $u = 1$ such states are not observed. Further disabling switching by increasing u would strongly reduce the number of coexisting species.

A value of $\Lambda \approx 0.03$ for the lower cutoff for the predator-prey size ratio is suggested by the evaluation of a large set of empirical data by Brose et al. (2006). The extension of the body mass range occupied by consumers sensitively depends on the exponent α that characterizes the decay of cacheability with large predator-prey mass ratios. With $\alpha = 0$, arbitrary large body sizes up to M_{max} are observed. With the parameter set used here, the choice $\alpha = 0.075$ restricts body masses to approximately $10 \,\text{kg}$.

---

[6] This ratio should not be confused with the ratio of producer production to respiration in the steady state, which is routinely measured.

A2.6   Model calibration

The reader will notice that some of the parameters listed in Tab. A1 have rather odd values, even though they are not directly based on empirical data. There are several reasons.

First, the way in which the parameter space is spanned in the computer model is slightly different from the way chosen here. For example, trophic niche widths had been expressed in therms of trophic niche densities $\sim w_t^{-D}, w_r^{-D}$, but this would here only confound notation.

Second, some parameter calibration is required in order to obtain a reasonable community structure in the steady state. It was attempted (i) to keep the numbers of producer and consumer species similar; (ii) to make sure that some consumers are omnivores *sensu stricto*, eating producers and consumers alike, while others are not (this can be achieved by controlling the ranges of vulnerability traits covered by producers and consumers in trophic niche space); (iii) to keep the fraction of top-predators around 0.2 as observed, (iv) to obtain a large number of trophic links per consumer, and (v) to have consumers cover a broad range of body masses, but to avoid producing a Loch Ness Monster or hitting $M_{\max}$.

Third, the computation time required to reach the steady state increases at least with the square of the number of species simulated. Simulations of systems with about 100 species per community take several days to reach the steady state. On the other hand, a large number of species is desired in order to reproduce collective, system-level ecological phenomena. Therefore, the steady-state number of species must be controlled in a narrow range. But the number of species appears to depend on most system parameters in a complicated way, and initial transients provide only little clues where it will ultimately settle in. Adjusting one parameter usually requires adjusting a second one in order to keep the number of species fixed, and the outcome is not always predictable.

Fourth, some parameter values were found to yield reasonable results at an earlier stage of model development, and were later kept fixed for simplicity.

Summarizing, much effort has been made to calibrate the model such as to obtain reasonable community structures within the computational limitations. The rational was that the demonstration of the top-down mechanism in a model that exhibits strong artifacts would not exclude the possibility that these artifacts were required for the mechanism to work. But in fact, rather the contrary seems to be true: Observations during the model calibration indicate that the requirements on parameters for the top-down mechanism to work are less restrictive than the requirement for achieving all the other community properties listed above.

References

Arditi, R., Michalski, J., 1995. Nonlinear food web models and their responses to increased basal productivity. In: Polis, G. A., Winemiller, K. O. (Eds.), Integration of Patterns and Dynamics. Chapman & Hall, London, pp. 122–133.

Berryman, A. A., Michalski, J., Gutierrez, A. P., Arditi, R., 1995. Logistic theory of food web dynamics. Ecology 76, 336–343.

Brose, U., Jonsson, T., Berlow, E. L., Warren, P., Banasek-Richter, C., Bersier, L.-F., Blanchard, J. L., Brey, T., Carpenter, S. R., Blandenier, M.-F. C., Cushing, L., Dawah, H. A., Dell, T., Edwards, F., Harper-Smith, S., Jacob, U., Ledger, M. E., Martinez, N. D., Memmott, J., Mintenbeck, K., Pinnegar, J. K., Rall, B. C., Rayner, T. S., Reuman, D. C., Ruess, L., Ulrich, W., Williams, R. J.,

Woodward, G., Cohen, J. E., 2006. Consumerresource body-size relationships in natural food webs. Ecology 87 (10), 2411–2417.

Claessen, D., van Oss, C., Roos, A. M., Persson, L., 2002. The impact of size-dependent predation on population dynamics and individual life history. Ecology 83 (6), 1660–1675.

Elliott, J. M., 2004. Prey switching in four species of carnivorous stoneflies. Freshwater Biology 49, 709–729.

Enquist, B. J., Brown, J. H., West, G. B., 1998. Allometric scaling of plant energetics and population density. Nature 395, 163–165.

Greenwood, J. J. D., Elton, R. A., 1979. Analysing experiments on frequency-dependent selection by predators. J. Anim. Ecol. 48, 721–737.

Hindmarsh, A. C., Brown, P. N., Grant, K. E., Lee, S. L., Serban, R., Shumaker, D. E., Woodward, C. S., 2005. SUNDIALS: Suite of Nonlinear and Differential/Algebraic Equation Solvers. ACM Trans. Math. Soft. 31 (3), 363–396.

Jeschke, J. M., Kopp, M., Tollrian, R., 2004. Consumer-food systems: why type I functional responses are exclusive to filter feeders. Biol. Rev. 79, 337–349.

McNiel, S., Lawton, J. H., 1970. Annual production and respiration in animal populations. Nature 225, 472–474.

Monsi, M., Saeki, T., 1953. Über den Lichtfaktor in den Pflanzengesellschaften und seine Bedeutung für die Stoffproduktion. Japanese Journal of Botany 14, 22–52.

Niklas, K. J., Enquist, B. J., 2001. Invariant scaling relationships for interspecific plant biomass production rates and body size. PNAS 98 (5), 2922–2927.

Peters, R. H., 1983. The ecological implications of body size. Cambridge University Press, Cambridge.

Rossberg, A. G., 2007. Part-whole relations between food webs and the validity of local food-web descriptions. Ecological Complexity Accepted.

Rossberg, A. G., Matsuda, H., Amemiya, T., Itoh, K., 2006. Food webs: Experts consuming families of experts. J. Theor. Biol. 241 (3), 552–563.

Savage, V. M., Gillooly, J. F., Brown, J. H., West, G. B., Charnov, E. L., 2004. Effects of body size and temperature on population growth. Am. Nat. 163 (3), 429–441.

Table A1: Model parameters and state variables

Symbol	Description	Important Equations	Range or Standard Value
A	system area		$1000\,\text{ha}$
M_i	body mass of species i	A.7	$M_{\min} \leq M_i \leq M_{\max}$
$M_{\min}$	smallest allowed body mass	A.7	$10^{-13}\,\text{kg}$
$M_{\max}$	largest allowed body mass	A.7	$10^3\,\text{kg}$
d	variation of body mass in speciations	A.7	3.0
M_0	allometric base unit		$1\,\text{kg}$
B_i	biomass of species i	A.1,A.5	$B_i \geq M_i$
ζ	general allometric exponent		-1/4
ζ_r	allometric exponent consumer metabolism		-1/4
T_i	resource "handling" time of consumer i	A.2,A.3,A.14	$T_i > 0$
a_i	attack rate of consumer i	A.2,A.3,A.11	$a_i > 0$
a_0	degeneration of attack rates in speciations	A.11	0.9
$\tilde{a}_0$	variation of attack rates in speciations	A.11	1.2
a_{start}	attack rate initializer	Sec. A1.5	$10^7\,\text{m}^2\text{kg}^{-1}\text{yr}^{-1}/A$
b_i	switching exponent of consumer i	A.2,A.3,A.12	see below
b_0	mean switching exponent	A.12	1.5
$\tilde{b}_0$	std switching exponent	A.12	0.3
u	resolution of resources when switching	A.3	1
ϵ	gross conversion efficiency	A.1,A.14	0.45
ϵ_0	net conversion efficiency	A.14	0.2
P/R	consumer production/respiration ratio	A.14	0.8
r_i	respiration rate of consumer i	A.1,A.14	$r_i > 0$
c_{ki}	trophic interaction coefficients	A.2,A.3,A.4	$c_{ki} > 0$
w_t	trophic niche width	A.4	0.446
α	small resource cutoff exponent	A.4	0.075
Λ	min predator-prey mean body mass ratio	A.4	0.03
$r_{\max,i}$	max population growth rate of consumer i	A.14	$0.81\,\text{yr}^{-1}(M_i/M_0)^{\zeta_r}$
$\text{GPP}_{\max}$	monoculture GPP	A.15	$10^3\,\text{kg}\,\text{yr}^{-1}\text{m}^{-2} \times A$
$\sigma_{\max,i}$	max population growth rate of producer i	Sec. A2.4	$0.208\,\text{yr}^{-1}(M_i/M_0)^{-1/4}$
l_i	loss rate of producer i	A.5	$\sigma_{\max,i}/9$
σ_i	gross population growth rate of producer i	A.5	$\sigma_{\max,i} + l_i$
d_{ij}	producer resource competition matrix	A.6	$d_{ij} > 0$
w_r	producer niche width	A.6	0.976
T_{SS}	max population-dynamical relaxation time	Sec. A1.6	$30\,\text{yr}$
D	dimensionality of niche spaces	Sec. A2.2	5
$\vec{V}_i$	vulnerability traits of species i	A.8	$\vec{V}_i \in \mathbf{R}^D$

Symbol	Description	Important Equations	Range or Standard Value
$\vec{F}_i$	foraging traits of consumer i	A.9	$\vec{F}_i \in \mathbf{R}^D$
$\vec{G}_i$	niche traits of producer i	A.10	$\vec{G}_i \in \mathbf{R}^D$
s	producer-consumer trait separation	A.8	1.4
σ_V	nominal variability of $\vec{V}_i$	A.8	0.2
σ_F	nominal variability of $\vec{F}_i$	A.9	3.0
σ_G	nominal variability of $\vec{G}_i$	A.10	1.0
μ_V	mutation of $\vec{V}_i$ in speciations	A.8	0.025
μ_F	mutation of $\vec{F}_i$ in speciations	A.9	6.0
μ_G	mutation of $\vec{G}_i$ in speciations	A.10	0.025
κ	invasion pressure	Sec. A1.4	1.4